

One-Dimensional Liquid ^4He : Dynamical Properties beyond Luttinger-Liquid Theory

G. Bertaina,¹ M. Motta,² M. Rossi,^{3,4,5} E. Vitali,² and D. E. Galli¹

¹*Dipartimento di Fisica, Università degli Studi di Milano, via Celoria 16, I-20133 Milano, Italy*

²*Department of Physics, The College of William and Mary, Williamsburg, Virginia 23187, USA*

³*Scuola Normale Superiore, Piazza dei Cavalieri 7, I-56126 Pisa, Italy*

⁴*International Center for Theoretical Physics (ICTP), Strada Costiera 11, I-34154 Trieste, Italy*

⁵*Dipartimento di Fisica e Astronomia, Università degli Studi di Padova, via Marzolo 8, I-35131 Padova, Italy*

(Received 22 December 2014; revised manuscript received 23 February 2016; published 1 April 2016)

We compute the zero-temperature dynamical structure factor of one-dimensional liquid ^4He by means of state-of-the-art quantum Monte Carlo and analytic continuation techniques. By increasing the density, the dynamical structure factor reveals a transition from a highly compressible critical liquid to a quasisolid regime. In the low-energy limit, the dynamical structure factor can be described by the quantum hydrodynamic Luttinger-liquid theory, with a Luttinger parameter spanning all possible values by increasing the density. At higher energies, our approach provides quantitative results beyond the Luttinger-liquid theory. In particular, as the density increases, the interplay between dimensionality and interaction makes the dynamical structure factor manifest a *pseudo-particle-hole* continuum typical of fermionic systems. At the low-energy boundary of such a region and moderate densities, we find consistency, within statistical uncertainties, with predictions of a power-law structure by the recently developed nonlinear Luttinger-liquid theory. In the quasisolid regime, we observe a novel behavior at intermediate momenta, which can be described by new analytical relations that we derive for the hard-rods model.

DOI: [10.1103/PhysRevLett.116.135302](https://doi.org/10.1103/PhysRevLett.116.135302)

One-dimensional (1D) quantum systems exhibit some of the most diverse and fascinating phenomena of condensed matter physics [1–3]. Among the most spectacular signatures of the interplay between quantum fluctuations, interaction and reduced dimensionality, are the breakdown of ordered phases in the presence of short-range interactions [4] and the loosened distinction between Bose and Fermi behavior [5]. The study of quasi-1D quantum systems is a very active research field, aroused by the experimental investigation of electronic transport properties [6–10], by the fabrication of long 1D arrays of Josephson junctions [11], and recently corroborated by the availability of ultracold atomic gases in highly anisotropic traps and optical lattices [2,12–14], as well as by experiments on confined He atoms [15–19].

The low-energy properties of a wide class of Bose and Fermi 1D quantum systems [1,20] are notoriously captured by the phenomenological Tomonaga-Luttinger-liquid (TLL) theory [21–23], characterized by collective phonon-like excitations. This theory introduces two conjugate Bose fields $\phi(x)$ and $\theta(x)$ describing, respectively, the density and phase fluctuations of the field operator $\psi(x) = \sqrt{\rho + \partial_x \phi(x)} e^{i\theta(x)}$, where ρ is the average density. Those fields are described by the exactly solvable low-energy effective Hamiltonian:

$$H_{LL} = \frac{\hbar}{2\pi} \int dx \left(c K_L \partial_x \theta(x)^2 + \frac{c}{K_L} \partial_x \phi(x)^2 \right). \quad (1)$$

Although, in general, the TLL parameter K_L and the sound velocity c are independent quantities (notably in lattice models), for Galilean-invariant systems $c = v_F/K_L$ [23], $v_F = \hbar k_F/m$ being the Fermi velocity and $k_F = \pi\rho$ the Fermi wave vector of a 1D ideal Fermi gas (IFG), and K_L is thus related to the compressibility κ_S by $mK_L^2 = \hbar^2 \pi^2 \rho^3 \kappa_S$. Such collective excitations are revealed by the low-momentum and low-energy behavior of the dynamical structure factor:

$$S(q, \omega) = \int dt \frac{e^{i\omega t}}{2\pi N} \langle e^{iHt/\hbar} \rho_q e^{-iHt/\hbar} \rho_{-q} \rangle, \quad (2)$$

where $\rho_q = \sum_{i=1}^N e^{iqx_i}$ is the Fourier transform of the density operator, N the number of particles, H the Hamiltonian, and x_i the position of the i th particle [24]. A complete characterization of density fluctuations requires one to compute (2) also beyond the limits of applicability of the TLL theory. A deep insight in the characterization of (2) at higher frequencies is provided by the phenomenological nonlinear TLL theory [3,25]; for integrable models, quantitative results are also provided by nonperturbative numeric calculations [13,14,26–28]. For physically relevant nonintegrable systems, on the other hand, the study of (2) requires more general approaches.

In this Letter, we probe the excitations of 1D liquid ^4He by evaluating its complete zero-temperature dynamical structure factor with fully *ab initio* methods. When strictly

confined in 1D, ^4He provides a spectacular condensed-matter realization of a TLL, having the unique feature of spanning all possible values of K_L by only varying the density. The interest in this system emerges also in connection with experimental realizations and theoretical characterizations of quasi-1D He systems confined inside nanopores [17,29–31] or moving inside dislocation lines in crystalline He samples [18,19,32]. A realistic microscopic description of the system is provided by the Hamiltonian

$$H = -\frac{\hbar^2}{2m} \sum_{i=1}^N \frac{\partial^2}{\partial x_i^2} + \sum_{i < j=1}^N V(x_i - x_j), \quad (3)$$

$V(x)$ being the well-established Aziz potential [33]. We access $S(q, \omega)$ by performing an inverse Laplace transform of the imaginary-time correlation function:

$$F(q, \tau) = \frac{1}{N} \langle e^{\tau H/\hbar} \rho_q e^{-\tau H/\hbar} \rho_{-q} \rangle = \int_0^\infty d\omega e^{-\tau\omega} S(q, \omega). \quad (4)$$

We compute $F(q, \tau)$ using the path integral ground state (PIGS) method [34,35], which provides unbiased [36] estimates of ground-state properties and imaginary-time correlations by statistically sampling the wave function $\Psi_\tau = e^{-\tau H} \Psi_T$, where Ψ_T is a trial state [37,38], non-orthogonal to the ground state of H . At sufficiently large τ , the expectation values over Ψ_τ are compatible with ground-state averages. We simulate up to $N = 160$ particles using periodic boundary conditions and find that our results are representative of the thermodynamic limit already for $N = 40$ particles within statistical uncertainty (see Supplemental Material [39]). Inverting the Laplace transform in Eq. (4) is notoriously an ill-posed inverse problem, meaning that many possible $S(q, \omega)$ are compatible with the imaginary-time data. However, a number of inversion strategies have provided reliable results for physically relevant systems [40–43]. In this Letter, we use the state-of-the-art genetic inversion via falsification of theories (GIFT) algorithm [43–50].

We study the Galilean-invariant liquid phase which is notoriously stable above the density $\rho_{\text{sp}} = 0.026(2) \text{ \AA}^{-1}$, where it undergoes a spinodal decomposition [51–53], namely, the formation of liquid droplets. In Fig. 1, we compute the TLL parameter K_L of the system as a function of $\rho > \rho_{\text{sp}}$ from both the compressibility and the sound velocity, inferred from the low-momentum behavior of the static structure factor $S(q) = F(q, 0) \approx K_L(q/2k_F)$. The good agreement between the two estimates over the whole density range confirms their accuracy and the internal consistency of our approach. Close to the spinodal decomposition, the sound velocity provides a more precise estimate of K_L [54]. As the density increases, K_L monotonically decreases from ∞ to 0, manifesting three fundamental regimes. At density $\rho \lesssim 0.06 \text{ \AA}^{-1}$, the system is in

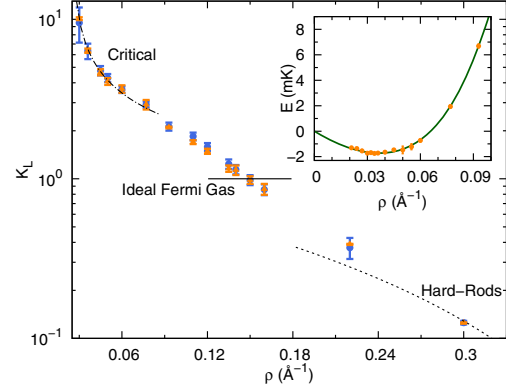


FIG. 1. TLL parameter K_L , from the compressibility $\kappa_S^{-1} = \rho \partial_\rho [\rho^2 \partial_\rho E(\rho)]$ (blue circles) and the low- q behavior of $S(q)$ (orange triangles). Superimposed lines are described in the text. Inset: Equation of state $E(\rho)$.

the spinodal critical regime, and we observe $K_L \propto (\rho - \rho_{\text{sp}})^{-\zeta}$ with $\zeta \approx 0.5$. This is equivalent to a dependence $c \propto (P - P_{\text{sp}})^\nu$ of sound velocity with the pressure difference $P - P_{\text{sp}}$, with P_{sp} the pressure at the spinodal point and $\nu = \zeta/(2\zeta + 1) \approx 0.25$, which is interestingly consistent with the critical value in three-dimensional helium [55–58]. At density $\rho \gtrsim 0.30 \text{ \AA}^{-1}$, we observe instead a good agreement with the hard-rods (HR) model [59], defined by $V(x) = \infty$ for $|x| < a$ and 0 otherwise. In Fig. 1, we take $a = 2.139 \text{ \AA}$, which is the scattering length of the repulsive part of the ^4He potential as in Ref. [60]. The HR model spans all values of $K_L = (1 - \rho a)^2 < 1$ as a function of the density. At the intermediate density $\rho \approx 0.150 \text{ \AA}^{-1}$, ^4He attains $K_L = 1$, which is the TLL parameter of the Tonks-Girardeau gas of impenetrable pointlike bosons [5] and of the 1D IFG.

The diverse behavior of ^4He is a peculiar consequence of the interplay between the hard-core repulsion, the van der Waals attraction in the interaction potential, and the mass of the atoms. It has been recently recognized that the TLL

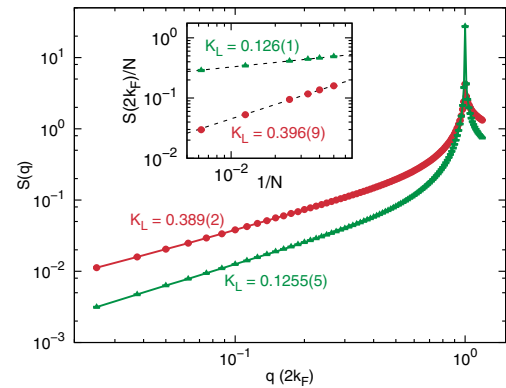


FIG. 2. Static structure factor $S(q)$ at $\rho = 0.22$ and 0.30 \AA^{-1} (red circles and green triangles, respectively). Inset: Scaling of $S(2k_F)$ with N at the same densities (dashed lines, fit to a power law). Values of K_L from c and the scaling of $S(2k_F)$ are reported.

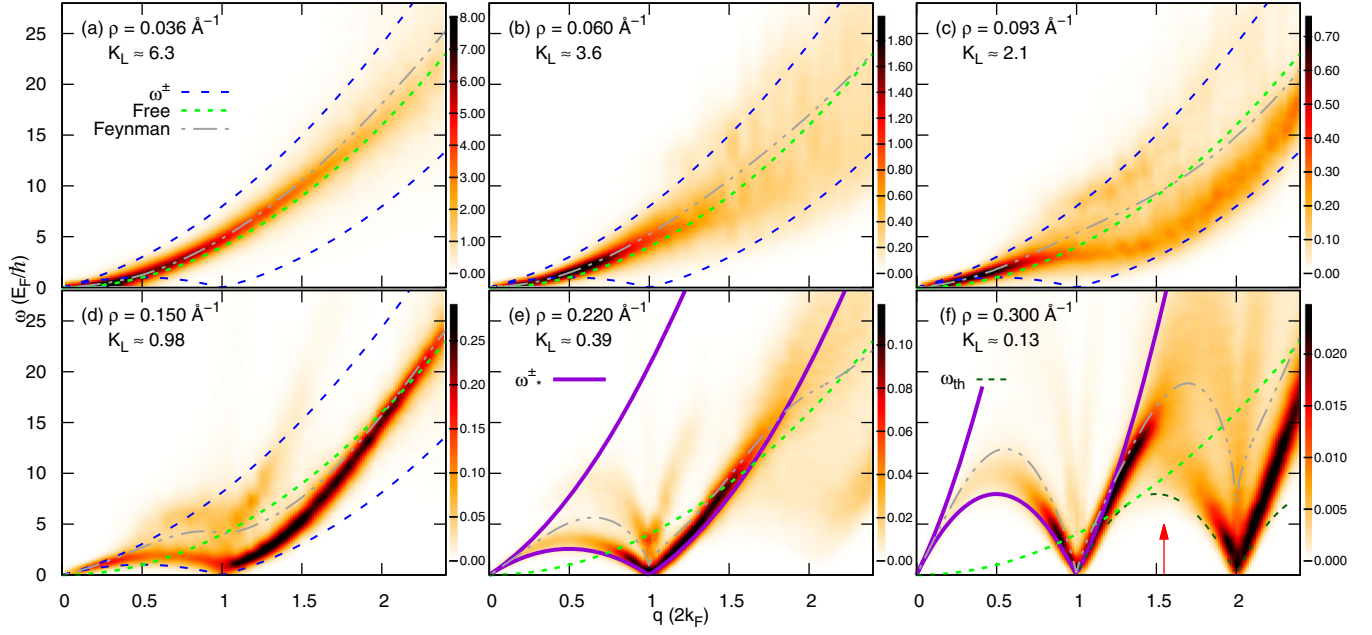


FIG. 3. Color plot of $S(q, \omega)$ at several densities and corresponding K_L . Feynman approximation $\omega_F(q)$ (gray dash-dotted lines) and the free-particle dispersion $\hbar q^2/2m$ (green dotted lines) are drawn for comparison. Panels (a)–(d) show also the bounds $\omega^\pm(q)$ of the particle-hole band (blue dashed line), while panels (e) and (f) show the bounds $\omega_\pm^*(q)$ of the HR elementary excitations (violet solid line). Panel (f) shows the low-energy threshold $\omega_{th}(q)$ of HR with $K_L = 0.125$ (double-dashed line) and momentum Q_1 (red arrow). Values of $S(q, \omega)$ beyond the scale are plotted in black.

parameter of ^3He features a similar high-density behavior [61]; the low-density behavior, however, is remarkably different, as the smaller mass of ^3He prevents a spinodal decomposition, maintaining K_L and the compressibility below a finite value.

In view of the universality of the TLL theory, knowledge of K_L sheds light on the low-momentum and low-energy structure of $S(q, \omega)$. The TLL theory also predicts [62–64] a power-law singularity $S(q = 2k_F j, \omega) \sim \omega^{2(j^2 K_L - 1)}$ for $\omega \rightarrow 0$ and integer ($j \in \mathbb{N}$) multiples of $2k_F$. Such a singularity is strictly related to the emergence of quasi-Bragg peaks in the static structure factor, featuring a sublinear growth $S(2k_F j) \propto N^{1-2j^2 K_L}$ [59] with the number of particles. The height of the j th peak diverges, in the thermodynamic limit, provided that $2j^2 K_L < 1$. In Fig. 2, we observe the emergence of quasi-Bragg peaks in $S(2k_F)$ at densities $\rho > 0.196(5) \text{ \AA}^{-1}$, where $K_L < 1/2$. This is naturally expected, since the small compressibility sets up a diagonal quasi-long-range order, while crystallization is prohibited by the dimensionality and by the range of the interaction [59]. The scaling of $S(2k_F)$ with N , reported in the inset in Fig. 2, provides an alternative estimate of K_L , in agreement with the results in Fig. 1.

The rich physical behavior suggested by the TLL parameter is notably unveiled by the dynamical structure factor, that our approach characterizes over the entire momentum-energy plane. Figure 3 shows $S(q, \omega)$ as a function of momentum and frequency, in Fermi units $2k_F$ and $E_F/\hbar = \hbar k_F^2/2m$, respectively, at several

representative densities. We show also Feynman’s approximation for the excitation spectrum $\omega_F(q) = \hbar q^2/2m S(q)$, which postulates a single mode saturating the f -sum rule $\hbar q^2/2m = \int d\omega S(q, \omega) \omega$. Departures from the Feynman spectrum indicate a broadening or the presence of multiple modes [65].

As expected, for small q and ω , $S(q, \omega)$ is always peaked around the phonon dispersion relation $\omega = cq$. On the other hand, the high-energy scenario is strikingly different and strongly dependent on the density. At $K_L \approx 6.3$ [Fig. 3(a)], the spectral weight is very close to the free-particle dispersion, consistent with similar predictions for 3D helium at negative pressures [55–58]. Such behavior is common to the Lieb-Liniger contact interaction model at large K_L [26,66,67], although in the case of ^4He the physical origin of such behavior lies in the spinodal critical point. At large momentum ($q \gtrsim k_F$) and energy, we observe a broadening of $S(q, \omega)$ that becomes more and more pronounced as K_L decreases [Figs. 3(b) and 3(c)]. As in the Lieb-Liniger model [26], the spectral weight of $S(q, \omega)$ partially fills the particle-hole band of the 1D IFG, enclosed between the dispersion relations $\omega^\pm(q) = |v_F q \pm \hbar q^2/2m|$. In both cases, this reveals a tendency for fermionization [5]: The repulsive interaction between 1D bosons mimics the Pauli exclusion principle and makes $S(q, \omega)$ manifest the particle-hole continuum typical of spinless free fermions. At $K_L \approx 2.1$ [Fig. 3(c)], the spectral weight of ^4He starts to concentrate again, emerging as a phonon and then bending downwards to approach $\omega^-(q)$. Such peculiar behavior is reminiscent

of the deflection of the Bogoliubov mode in 3D systems of hard spheres [50,68], with the notable difference that in 1D the spectral weight at $q \approx 2k_F j$ is nonzero up to very low frequency. At $K_L \approx 1$ [Fig. 3(d)], the incipient concentration of the spectral weight becomes strikingly manifest and takes place around a low-energy excitation, which is close to $\omega^-(q)$ for $q < 2k_F$ and approaches the free-particle dispersion relation for higher momentum. However, $S(2k_F, \omega)$ is almost flat at low frequency $\omega \lesssim E_F/\hbar$, within our resolution (see Supplemental Material [39]), analogously to the Tonks-Girardeau and IFG models. Above the low-energy excitation, a lower-intensity secondary structure overhangs; for $K_L < 1$ [Figs. 3(e) and 3(f)], it evolves into a well-defined high-energy structure attaining a nonzero local minimum at $q = 2k_F$, in correspondence of the free-particle energy. Although a precise characterization of this structure requires further investigation, it is reminiscent of a 3D rotonic behavior or of multiphonons [50,68–70]. For $K_L \approx 0.39$ [Fig. 3(e)], $S(q, \omega)$ is mostly distributed in a region with boundaries $\omega_\pm^*(q)$, which are modified with respect to $\omega^\pm(q)$ as an effect of interaction, and the spectral weight concentrates close to the lower branch $\omega_-^*(q)$. We notice that $\omega_\pm^*(q) = \omega^\pm(q)/K_L$ [solid lines in Figs. 3(e) and 3(f)]. A similar behavior can be discerned [71] in the super-Tonks-Girardeau gas [72,73], a gaseous excited state of the attractive Lieb-Liniger model. This behavior can be quantitatively explained: In the high-density regime, the main interaction effect is volume exclusion, as in the HR model. The solution of such a model via the Bethe ansatz technique [74–76] shows that the eigenfunctions of the HR Hamiltonian can be mapped onto those of an IFG with increased density $\rho/(1 - \rho a)$, thus yielding a scaling factor $(1 - \rho a)^{-2} = K_L^{-1}$ in the boundaries of the particle-hole band.

The distribution of spectral weight changes dramatically for $K_L \approx 0.125$ [Fig. 3(f)] for $2k_F < q < 4k_F$, where the low-energy excitation rapidly broadens and flattens at $q \approx 3.2k_F$ and concentrates again at a lower energy around $q \approx 4k_F$. A quantitative explanation of this effect can be given in the light of the recently developed nonlinear TLL theory [3], again modeling ^4He atoms with HR. The nonlinear TLL theory assumes the existence of a low-energy threshold $\omega_{\text{th}}(q)$, below which no excitations are present. Interpreting an excitation with frequency $\omega \gtrsim \omega_{\text{th}}(q)$ as the creation of a mobile impurity in an otherwise usual TLL, the nonlinear TLL theory shows that $S(q, \omega)$ features a power-law singularity:

$$S(q, \omega) \propto \Theta(\omega - \omega_{\text{th}}(q)) |\omega - \omega_{\text{th}}(q)|^{-\lambda(q)}, \quad (5)$$

where $\lambda(q)$ is a function of K_L and $\omega_{\text{th}}(q)$ [25] and $\Theta(\omega)$ is the Heaviside step function. The expansion $\omega_{\text{th}}(q) \approx cq - \hbar q^2/2m^*$ of the low-energy threshold around $q = 0$ defines the effective mass m^* , which sets the energy scale where modifications from the TLL theory take place [25]. The effective mass is a function $1/m^* = c\partial_\mu(c\sqrt{K_L})/K_L$ of K_L

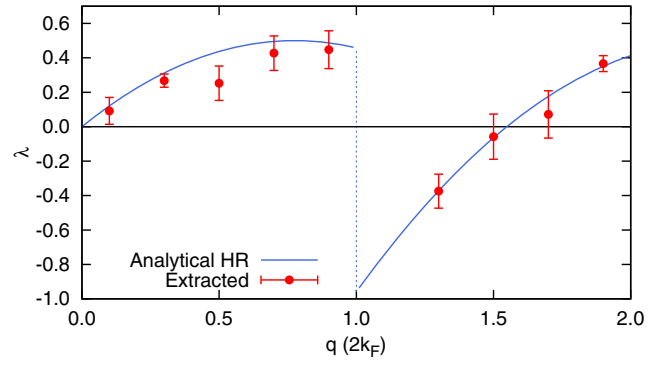


FIG. 4. Analytical nonlinear TLL exponent Eq. (6) for HR with $K_L = 0.125$ (solid line) and PIGS + GIFT (circles) fitted exponents of ^4He at density $\rho = 0.3 \text{ \AA}^{-1}$.

and the chemical potential μ [25,77]. For the HR model we indeed derive $m/m^* = 1/K_L$, indicating that $\omega_{\text{th}}(q) \approx \omega_-^*(q)$ for small momentum. This is again confirmed over the whole range $0 \leq q \leq 2k_F$ by the analytical solution of the HR model [76]. Away from this basic region, the low-energy threshold repeats periodically [3,63,78] as shown in Fig. 3(f); therefore, $\omega_{\text{th}}(q) = \omega_-^*(q - 2nk_F)$ with $2nk_F < q < 2(n+1)k_F$ and n integer.

For the HR model, given the analytic expressions of K_L and $\omega_{\text{th}}(q)$, we extract the exponents following Ref. [25]:

$$\lambda(q) = -2(\tilde{q} - n)(\tilde{q} - n - 1), \quad \tilde{q} \equiv qa/2\pi. \quad (6)$$

In Fig. 4, we show $\lambda(q)$ for a HR system with the same K_L as in Fig. 3(f), comparing it to numerically extracted exponents as described below. $\lambda(q)$ is a piecewise continuous function of q , with jump singularities at $q = 2nk_F$. For $0 \leq q < 2k_F$, $\lambda(q) > 0$ and $S(q, \omega)$ diverges close to $\omega_{\text{th}}(q)$. After $q = 2k_F$, $\lambda(q)$ changes sign, and thus $S(q, \omega)$ vanishes close to $\omega_{\text{th}}(q)$. In fact, for $2k_F < q \lesssim 3.2k_F$, the spectral weight concentrates much above $\omega_{\text{th}}(q)$, around $\omega_-^*(q)$, a feature which is even beyond the nonlinear TLL theory. Equation (6) predicts a flat $S(q, \omega)$ at the special wave vectors $Q_n = 2\pi n/a$, consistent with a previous result [59] based on exact properties of the HR model. We indeed observe almost flat $S(q, \omega)$ at $Q_1 = 3.24k_F \approx 2\pi/a$ [red arrow in Fig. 3(f)]. Beyond Q_1 , the divergence reappears, since $\lambda(q) < 0$.

To quantitatively verify prediction (6), for some momenta we have performed much more refined reconstructions at $\rho = 0.3 \text{ \AA}^{-1}$, imposing $S(q, \omega) = 0$ [79] below the exact $\omega_{\text{th}}(q)$ for the HR model and fitting the obtained spectrum to a power law (see Supplemental Material [39]). The obtained exponents are indicated in Fig. 4: This procedure does not disprove the power-law model (5) in a range of frequencies up to $\sim \omega_{\text{th}}(q) + E_F/\hbar$, depending on momentum [80] and yields exponents $\lambda(q)$ which are consistent with the nonlinear TLL prediction (6) within statistical uncertainty. This result is quite

remarkable, since no prior knowledge about $S(q, \omega)$ has been enforced in the analytic continuations, except for the f -sum rule and the exact threshold for HR [81].

We have thus provided a robust description of the system in the experimentally relevant high-density regime, based on the HR model, which almost fully characterizes the spectrum at low and intermediate energies. The novel structure predicted around momenta that are multiples of $2\pi/a$ is relevant, and would be very interesting to experimentally observe, for all quantum excluded-volume systems, such as liquid He inside nanopores, Rydberg gases [82,83], and super-Tonks-Girardeau gases.

We acknowledge very useful discussions with G. Astrakharchik. We are grateful to A. Parola for revising the manuscript. We thank M. Panfil and coauthors for providing us with their data on the super-Tonks-Girardeau gas. The simulations were performed on the supercomputing facilities at CINECA and at the Physics Departments of the Universities of Milan and Padua. We thank the Computing Support Staff at INFN and Physics Department of the University of Milan. We acknowledge the CINECA and the Regione Lombardia award LI03p-UltraQMC, under the LISA initiative, for the availability of high-performance computing resources and support. M.M. acknowledges funding from the Dr. Davide Colosimo Award, celebrating the memory of physicist Davide Colosimo. M.M. and E.V. acknowledge support from the Physics Department of the University of Milan, the Simons Foundation, and NSF (Grant No. DMR-1409510). G.B. and D.E.G. acknowledge funding from D.E. Pini.

-
- [1] T. Giamarchi, *Quantum Physics in One Dimension* (Oxford University Press, New York, 2003).
 - [2] M. A. Cazalilla, R. Citro, T. Giamarchi, E. Orignac, and M. Rigol, One dimensional bosons: From condensed matter systems to ultracold gases, *Rev. Mod. Phys.* **83**, 1405 (2011).
 - [3] A. Imambekov, T. L. Schmidt, and L. I. Glazman, One-dimensional quantum liquids: Beyond the Luttinger liquid paradigm, *Rev. Mod. Phys.* **84**, 1253 (2012).
 - [4] N. D. Mermin and H. Wagner, Absence of Ferromagnetism or Antiferromagnetism in One- or Two-Dimensional Isotropic Heisenberg Models, *Phys. Rev. Lett.* **17**, 1133 (1966).
 - [5] M. Girardeau, Relationship between systems of impenetrable bosons and fermions in one dimension, *J. Math. Phys. (N.Y.)* **1**, 516 (1960).
 - [6] A. M. Chang, L. N. Pfeiffer, and K. W. West, Observation of Chiral Luttinger Behavior in Electron Tunneling into Fractional Quantum Hall Edges, *Phys. Rev. Lett.* **77**, 2538 (1996).
 - [7] Z. Yao, H. W. Ch. Postma, L. Balents, and C. Dekker, Carbon nanotube intramolecular junctions, *Nature (London)* **402**, 273 (1999).
 - [8] M. Bockrath, D. H. Cobden, J. Lu, A. G. Rinzler, R. E. Smalley, L. Balents, and P. L. McEuen, Luttinger-liquid behaviour in carbon nanotubes, *Nature (London)* **397**, 598 (1999).
 - [9] A. N. Aleshin, H. J. Lee, Y. W. Park, and K. Akagi, One-Dimensional Transport in Polymer Nanofibers, *Phys. Rev. Lett.* **93**, 196601 (2004).
 - [10] S. V. Zaitsev-Zotov, Y. A. Kumzerov, Y. A. Firsov, and P. Monceau, Luttinger-liquid-like transport in long InSb nanowires, *J. Phys. Condens. Matter* **12**, L303 (2000).
 - [11] E. Chow, P. Delsing, and D. B. Haviland, Length-Scale Dependence of the Superconductor-to-Insulator Quantum Phase Transition in One Dimension, *Phys. Rev. Lett.* **81**, 204 (1998).
 - [12] I. Bloch and W. Zwerger, Many-body physics with ultracold gases, *Rev. Mod. Phys.* **80**, 885 (2008).
 - [13] N. Fabbri, M. Panfil, D. Clément, L. Fallani, M. Inguscio, C. Fort, and J.-S. Caux, Dynamical structure factor of one-dimensional Bose gases: Experimental signatures of beyond-Luttinger-liquid physics, *Phys. Rev. A* **91**, 043617 (2015).
 - [14] F. Meinert, M. Panfil, M. J. Mark, K. Lauber, J.-S. Caux, and H.-C. Nägerl, Probing the Excitations of a Lieb-Liniger Gas from Weak to Strong Coupling, *Phys. Rev. Lett.* **115**, 085301 (2015).
 - [15] B. Yager, J. Nyéki, A. Casey, B. P. Cowan, C. P. Lusher, and J. Saunders, NMR Signature of One-Dimensional Behavior of ^3He in Nanopores, *Phys. Rev. Lett.* **111**, 215303 (2013).
 - [16] M. Savard, G. Dauphinais, and G. Gervais, Hydrodynamics of Superfluid Helium in a Single Nanohole, *Phys. Rev. Lett.* **107**, 254501 (2011).
 - [17] J. Taniguchi, K. Demura, and M. Suzuki, Dynamical superfluid response of ^4He confined in a nanometer-size channel, *Phys. Rev. B* **88**, 014502 (2013).
 - [18] Y. Vekhov and R. B. Hallock, Mass Flux Characteristics in Solid ^4He for $T > 100$ mK: Evidence for Bosonic Luttinger-Liquid Behavior, *Phys. Rev. Lett.* **109**, 045303 (2012).
 - [19] Ye. Vekhov and R. B. Hallock, Dissipative superfluid mass flux through solid ^4He , *Phys. Rev. B* **90**, 134511 (2014).
 - [20] G. F. Giuliani and G. Vignale, *Quantum Theory of the Electron Liquid* (Cambridge University Press, Cambridge, England, 2005).
 - [21] S.-I. Tomonaga, Remarks on Bloch's method of sound waves applied to many-fermion problems, *Prog. Theor. Phys.* **5**, 544 (1950).
 - [22] J. M. Luttinger, An exactly soluble model of a many-fermion system, *J. Math. Phys. (N.Y.)* **4**, 1154 (1963).
 - [23] F. D. M. Haldane, Effective Harmonic-Fluid Approach to Low-Energy Properties of One-Dimensional Quantum Fluids, *Phys. Rev. Lett.* **47**, 1840 (1981).
 - [24] Such a quantity is related to the imaginary part of the density-density response function by the fluctuation-dissipation theorem. See R. Kubo, The fluctuation-dissipation theorem, *Rep. Prog. Phys.* **29**, 255 (1966).
 - [25] A. Imambekov and L. I. Glazman, Phenomenology of One-Dimensional Quantum Liquids Beyond the Low-Energy Limit, *Phys. Rev. Lett.* **102**, 126405 (2009).
 - [26] J.-S. Caux and P. Calabrese, Dynamical density-density correlations in the one-dimensional Bose gas, *Phys. Rev. A* **74**, 031605 (2006).
 - [27] M. Mourigal, M. Enderle, A. Klöpperpieper, J.-S. Caux, A. Stunault, and H. M. Rønnow, Fractional spinon excitations

- in the quantum Heisenberg antiferromagnetic chain, *Nat. Phys.* **9**, 435 (2013).
- [28] B. Lake, D. A. Tennant, J.-S. Caux, T. Barthel, U. Schollwöck, S. E. Nagler, and C. D. Frost, Multispinon Continua at Zero and Finite Temperature in a Near-Ideal Heisenberg Chain, *Phys. Rev. Lett.* **111**, 137205 (2013).
- [29] C. T. Kresge, M. E. Leonowicz, W. J. Roth, J. C. Vartuli, and J. S. Beck, Ordered mesoporous molecular sieves synthesized by a liquid-crystal template mechanism, *Nature (London)* **359**, 710 (1992).
- [30] A. Del Maestro and I. Affleck, Interacting bosons in one dimension and the applicability of Luttinger-liquid theory as revealed by path-integral quantum Monte Carlo calculations, *Phys. Rev. B* **82**, 060515 (2010).
- [31] A. Del Maestro, M. Boninsegni, and I. Affleck, ^4He Luttinger Liquid in Nanopores, *Phys. Rev. Lett.* **106**, 105303 (2011).
- [32] M. Boninsegni, A. B. Kuklov, L. Pollet, N. V. Prokof'ev, B. V. Svistunov, and M. Troyer, Luttinger Liquid in the Core of a Screw Dislocation in Helium-4, *Phys. Rev. Lett.* **99**, 035301 (2007).
- [33] R. A. Aziz, V. P. S. Nain, J. S. Carley, W. L. Taylor, and G. T. McConville, An accurate intermolecular potential for helium, *J. Chem. Phys.* **70**, 4330 (1979).
- [34] A. Sarsa, K. E. Schmidt, and W. R. Magro, A path integral ground state method, *J. Chem. Phys.* **113**, 1366 (2000).
- [35] D. E. Galli and L. Reatto, Recent progress in simulation of the ground state of many boson systems, *Mol. Phys.* **101**, 1697 (2003).
- [36] M. Rossi, M. Nava, L. Reatto, and D. E. Galli, Exact ground state Monte Carlo method for Bosons without importance sampling, *J. Chem. Phys.* **131**, 154108 (2009).
- [37] L. Reatto and G. V. Chester, Phonons and the Properties of a Bose System, *Phys. Rev.* **155**, 88 (1967).
- [38] S. Vitiello, K. Runge, and M. H. Kalos, Variational Calculations for Solid and Liquid ^4He with a "Shadow" Wave Function, *Phys. Rev. Lett.* **60**, 1970 (1988).
- [39] See Supplemental Material at <http://link.aps.org/supplemental/10.1103/PhysRevLett.116.135302> for details on the PIGS and GIFT methods and examples of fits of the spectra at given momenta.
- [40] A. W. Sandvik, Stochastic method for analytic continuation of quantum Monte Carlo data, *Phys. Rev. B* **57**, 10287 (1998).
- [41] A. S. Mishchenko, N. V. Prokof'ev, A. Sakamoto, and B. V. Svistunov, Diagrammatic quantum Monte Carlo study of the Fröhlich polaron, *Phys. Rev. B* **62**, 6317 (2000).
- [42] D. R. Reichman and E. Rabani, Analytic continuation average spectrum method for quantum liquids, *J. Chem. Phys.* **131**, 054502 (2009).
- [43] E. Vitali, M. Rossi, L. Reatto, and D. E. Galli, *Ab initio* low-energy dynamics of superfluid and solid ^4He , *Phys. Rev. B* **82**, 174510 (2010).
- [44] M. Rossi, E. Vitali, L. Reatto, and D. E. Galli, Microscopic characterization of overpressurized superfluid ^4He , *Phys. Rev. B* **85**, 014525 (2012).
- [45] S. Saccani, S. Moroni, E. Vitali, and M. Boninsegni, Bose soft discs: A minimal model for supersolidity, *Mol. Phys.* **109**, 2807 (2011).
- [46] S. Saccani, S. Moroni, and M. Boninsegni, Excitation Spectrum of a Supersolid, *Phys. Rev. Lett.* **108**, 175301 (2012).
- [47] M. Nava, D. E. Galli, M. W. Cole, and L. Reatto, Superfluid state of ^4He on graphane and graphene-fluoride: Anisotropic roton states, *J. Low Temp. Phys.* **171**, 699 (2013).
- [48] M. Nava, D. E. Galli, S. Moroni, and E. Vitali, Dynamic structure factor for ^3He in two dimensions, *Phys. Rev. B* **87**, 144506 (2013).
- [49] F. Arrigoni, E. Vitali, D. E. Galli, and L. Reatto, Excitation spectrum in two-dimensional superfluid ^4He , *Low Temp. Phys.* **39**, 793 (2013).
- [50] R. Rota, F. Tramonto, D. E. Galli, and S. Giorgini, Quantum Monte Carlo study of the dynamic structure factor in the gas and crystal phase of hard-sphere bosons, *Phys. Rev. B* **88**, 214505 (2013).
- [51] G. Stan, V. H. Crespi, M. W. Cole, and M. Boninsegni, Interstitial He and Ne in nanotube bundles, *J. Low Temp. Phys.* **113**, 447 (1998).
- [52] E. Krotscheck and M. D. Miller, Properties of ^4He in one dimension, *Phys. Rev. B* **60**, 13038 (1999).
- [53] M. Boninsegni and S. Moroni, Ground state of ^4He in one dimension, *J. Low Temp. Phys.* **118**, 1 (2000).
- [54] Estimating K_L from κ_S requires differentiation of the equation of state, which is fitted to a polynomial. Uncertainties on the fit parameters propagate to κ_S , resulting in unavoidably large error bars near the spinodal decomposition, where the compressibility diverges.
- [55] F. Albergamo, J. Bossy, P. Averbuch, H. Schober, and H. R. Glyde, Phonon-Roton Excitations in Liquid ^4He at Negative Pressures, *Phys. Rev. Lett.* **92**, 235301 (2004).
- [56] M. A. Solís and J. Navarro, Liquid ^4He and ^3He at negative pressure, *Phys. Rev. B* **45**, 13080 (1992).
- [57] J. Boronat, J. Casulleras, and J. Navarro, Monte Carlo calculations for liquid ^4He at negative pressure, *Phys. Rev. B* **50**, 3427 (1994).
- [58] G. H. Bauer, D. M. Ceperley, and N. Goldenfeld, Path-integral Monte Carlo simulation of helium at negative pressures, *Phys. Rev. B* **61**, 9055 (2000).
- [59] F. Mazzanti, G. E. Astrakharchik, J. Boronat, and J. Casulleras, Ground-State Properties of a One-Dimensional System of Hard Rods, *Phys. Rev. Lett.* **100**, 020401 (2008).
- [60] See M. Kalos, D. Levesque, and L. Verlet, Helium at zero temperature with hard-sphere and other forces, *Phys. Rev. A* **9**, 2178 (1974). Note that, due to the hard core, the 1D scattering problem has the same boundary condition as the 3D reduced radial solution.
- [61] G. E. Astrakharchik and J. Boronat, Luttinger-liquid behavior of one-dimensional ^3He , *Phys. Rev. B* **90**, 235439 (2014).
- [62] A. Luther and I. Peschel, Single-particle states, Kohn anomaly, and pairing fluctuations in one dimension, *Phys. Rev. B* **9**, 2911 (1974).
- [63] A. H. Castro Neto, H. Q. Lin, Y.-H. Chen, and J. M. P. Carmelo, Pseudoparticle-operator description of an interacting bosonic gas, *Phys. Rev. B* **50**, 14032 (1994).
- [64] G. E. Astrakharchik and L. P. Pitaevskii, Motion of a heavy impurity through a Bose-Einstein condensate, *Phys. Rev. A* **70**, 013608 (2004).
- [65] A pioneering, but less general, fit of imaginary-time density correlations was performed for the dipolar gas in S. De Palo, E. Orignac, R. Citro, and M. L. Chiofalo, Low-energy excitation spectrum of one-dimensional dipolar quantum gases, *Phys. Rev. B* **77**, 212101 (2008).

- [66] E. H. Lieb and W. Liniger, Exact Analysis of an Interacting Bose Gas. I. The General Solution and the Ground State, *Phys. Rev.* **130**, 1605 (1963).
- [67] E. H. Lieb, Exact Analysis of an Interacting Bose Gas. II. The Excitation Spectrum, *Phys. Rev.* **130**, 1616 (1963).
- [68] M. Rossi and L. Salasnich, Path-integral ground state and superfluid hydrodynamics of a bosonic gas of hard spheres, *Phys. Rev. A* **88**, 053617 (2013).
- [69] R. A. Cowley and A. D. B. Woods, Inelastic scattering of thermal neutrons from liquid helium, *Can. J. Phys.* **49**, 177 (1971).
- [70] D. E. Galli, E. Cecchetti, and L. Reatto, Rotons and Roton Wave Packets in Superfluid ^4He , *Phys. Rev. Lett.* **77**, 5401 (1996).
- [71] We analyzed data from M. Panfil, J. De Nardis, and J.-S. Caux, Metastable Criticality and the Super Tonks-Girardeau Gas, *Phys. Rev. Lett.* **110**, 125302 (2013).
- [72] G. E. Astrakharchik, J. Boronat, J. Casulleras, and S. Giorgini, Beyond the Tonks-Girardeau Gas: Strongly Correlated Regime in Quasi-One-Dimensional Bose Gases, *Phys. Rev. Lett.* **95**, 190407 (2005).
- [73] E. Haller, M. Gustavsson, M. J. Mark, J. G. Danzl, R. Hart, G. Pupillo, and H.-C. Nägerl, Realization of an excited, strongly correlated quantum gas phase, *Science* **325**, 1224 (2009).
- [74] T. Nagamiya, Statistical mechanics of one-dimensional substances I, *Proc. Phys. Math. Soc. Jpn.* **22**, 705 (1940).
- [75] B. Sutherland, Quantum many-body problem in one dimension: thermodynamics, *J. Math. Phys. (N.Y.)* **12**, 251 (1971).
- [76] M. Motta, G. Bertaina, M. Rossi, E. Vitali, and D. E. Galli (to be published).
- [77] R. G. Pereira, J. Sirker, J.-S. Caux, R. Hagemans, J. M. Maillet, S. R. White, and I. Affleck, Dynamical Spin Structure Factor for the Anisotropic Spin-1/2 Heisenberg Chain, *Phys. Rev. Lett.* **96**, 257202 (2006).
- [78] A. Y. Cherny, J.-S. Caux, and J. Brand, Theory of superfluidity and drag force in the one-dimensional Bose gas, *Front. Phys.* **7**, 54 (2012).
- [79] A. W. Sandvik, Constrained sampling method for analytic continuation, [arXiv:1502.06066](https://arxiv.org/abs/1502.06066).
- [80] The calculation of $\lambda(q)$ at momenta slightly larger than $2k_F$ and $4k_F$ was prevented by the difficulty of resolving a vanishing spectrum in a narrow frequency range below the dominant higher-energy peak.
- [81] A small discrepancy is seen around $q = k_F$, where, in fact, the threshold for ^4He seems to be higher than that predicted by the HR model.
- [82] H. Schempp, G. Günter, M. Robert-de-Saint-Vincent, C. S. Hofmann, D. Breyel, A. Komnik, D. W. Schönleber, M. Gärtner, J. Evers, S. Whitlock, and M. Weidemüller, Full Counting Statistics of Laser Excited Rydberg Aggregates in a One-Dimensional Geometry, *Phys. Rev. Lett.* **112**, 013002 (2014).
- [83] P. Schauß, M. Cheneau, M. Endres, T. Fukuhara, S. Hild, A. Omran, T. Pohl, C. Gross, S. Kuhr, and I. Bloch, Observation of spatially ordered structures in a two-dimensional Rydberg gas, *Nature (London)* **491**, 87 (2012).